

**Molecular Cell, Volume 77**

**Supplemental Information**

**Functional Translatome Proteomics Reveal  
Converging and Dose-Dependent Regulation  
by mTORC1 and eIF2 $\alpha$**

**Kevin Klann, Georg Tascher, and Christian Münch**

## SUPPLEMENTARY FIGURE LEGENDS

### **Figure S1. mePROD accurately determines acute changes in relative protein translation rates, Related to Figure 1**

(A-B) Ratio compression of mePROD measurements. Comparison of samples from Figure 2 measured using MS<sup>2</sup> or MS<sup>3</sup> methods (A) and with or without noise subtraction employing the noise channel (B).

(C) Depiction of median measured relative translation rates (heavy/total) across time points (Figure 2H) relative to the determined dynamic range of mePROD (Figure 2E).

(D) Reproducibility of translation values for individual protein across different time points (Figure 2H). For each time-point, measured translation values were scaled between 0 and 1 and individual scaled translation values as well as calculated curve fits were plotted.

### **Figure S2. Assessment of quality of mePROD measurements, Related to Figure 3**

(A) Heatmap showing correlation between all replicates. Pearson correlation matrix was calculated and plotted. Tg, thapsigargin.

(B) Distribution of fold changes between DMSO or thapsigargin treated samples.

(C) Distribution of adjusted *P* values between DMSO or thapsigargin treated samples. Raw *P* values were calculated using two-sided, unpaired student's t-test (*n*=3) and FDR-corrected by the Benjamini Hochberg procedure.

### **Figure S3. Validation translation targets by comparison to existing ribosome profiling studies, Related to Figure 3**

(A) Comparison of Ribo-seq and mePROD translation data after activation of the integrated stress response. Plotted are the fractions of proteins overlapping between the Ribo-seq (indicated publications as below) and mePROD data sets (Figure 3).

(B, C) Histograms of relative translation rate fold changes observed by mePROD or Ribo-seq data from (Reid et al., 2014) (B), or (Paolini et al., 2018) (C).

### **Figure S4. Effect of endoplasmic reticulum stress on the functional translome, Related to Figure 3/4**

(A) Venn diagram showing the overlap between proteins with reduced translation in thapsigargin versus DMSO or thapsigargin+ISRIB treated cells (fold change (log<sub>2</sub>) < -0.5).

(B) Relative GO term associations for the whole quantified translome dataset compared to proteins with decreased translation (fold change < -0.5) upon thapsigargin treatment.

(C) Volcano plot showing translation rate fold changes of thapsigargin (Tg) and ISRIB versus DMSO treated cells and statistical significance. Raw *P* values were calculated using two-sided,

unpaired student's t-test ( $n=3$ ) and FDR-corrected by the Benjamini Hochberg procedure. Significantly changing proteins are marked in orange.

(D) GO term network analysis of translome changes upon thapsigargin treatment showing proteins with unchanged (orange) or decreased (blue, fold change  $< -0.5$ ) translation.

(E) Scheme of Mannose-6-phosphate receptor (MPR) trafficking in cells and the effect of thapsigargin on the pathway. Shown are thapsigargin/control fold changes ( $\log_2$ ) for the main pathway components.

### **Figure S5. Overlap of proteins with reduced translation after folding-, oxidative-, or osmotic stress, Related to Figure 4**

(A) Venn-diagram showing overlap between proteins showing significant translation decrease (fold change  $< -0.5$ , adjusted  $P$  value  $< 0.05$ ) upon treatment with thapsigargin, NaCl, or arsenite. Only proteins detected in all datasets are shown.

(B) Western blot showing eIF2 $\alpha$  (total EIF2S1) and P-eIF2 $\alpha$  (P-EIF2S1) levels upon control, NaCl or arsenite treatments for 2.5 h with or without ISRIB co-treatment.

(C) Venn diagram showing proteins whose translation attenuation after arsenite (Ars), NaCl, or thapsigargin (Tg) treatment could be rescued by addition of ISRIB (Fold change  $> 0.5$ ).

(D) Transcriptional fold changes extracted from previously published datasets following UPR induction (Paolini et al., 2018), arsenite treatment (Andreev et al., 2015), or pharmacological mTOR inhibition (Thoreen et al., 2012) were plotted. Median fold changes are indicated on top.

(E–G) Transcriptional fold changes from datasets used in (D) plotted against mePROD translation data (Figure 4). Pearson correlation values are indicated within the figures. Ctrl, control. FC, fold change.

### **Figure S6. Translation behavior of different protein clusters during 4EGI titration, Related to Figure 6**

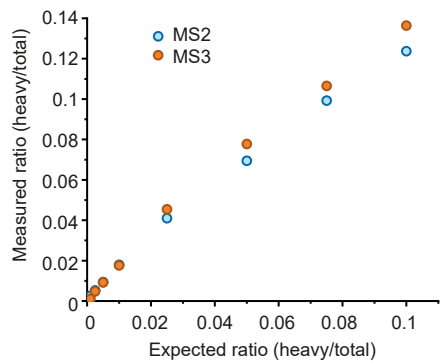
(A) Cluster profiles of the two main clusters identified from Figure 6F. Z scores were plotted for each sample. Greyscale indicates distance from the cluster center. Dashed line indicates linear reference line.

(B) Translation rates of all proteins present in dataset were normalized to control sample and linear fitting carried out. All individual proteins ( $n=2,190$ ) following the linear fit with a  $P$  value lower than 0.05 were plotted. The dashed line represents the averaged curve.

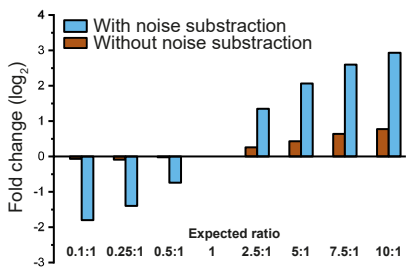
(C) Reactome FI network of proteins retaining their translational status over all tested 4EGI concentrations.

Figure S1

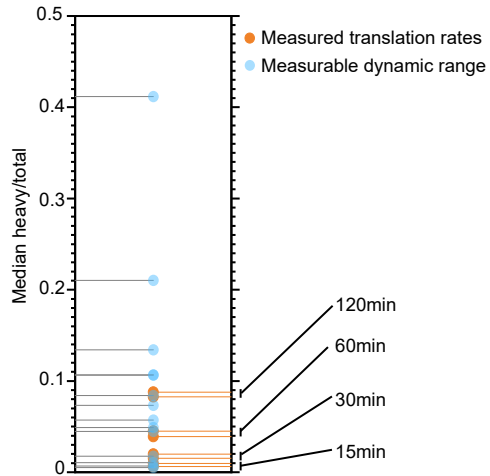
**A**



**B**



**C**



**D**

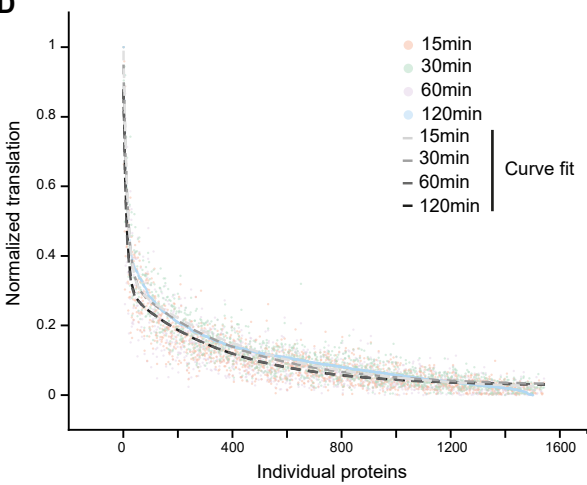
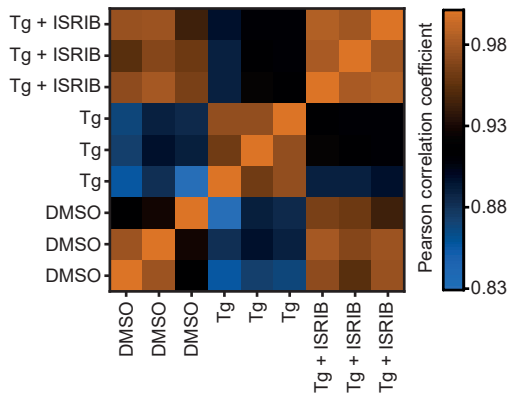
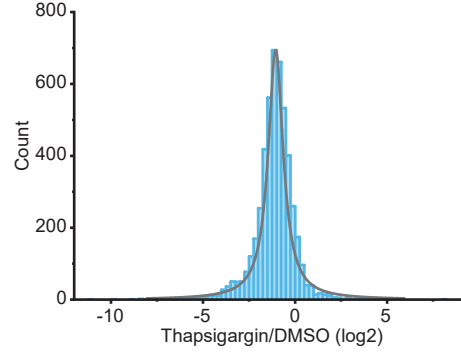


Figure S2

**A**



**B**



**C**

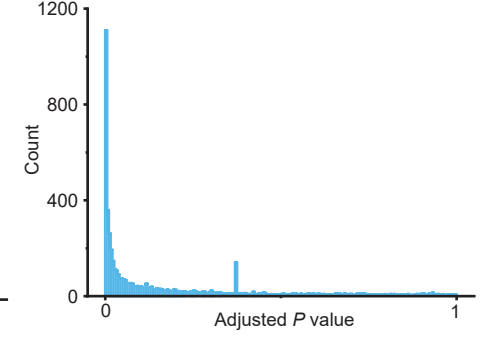
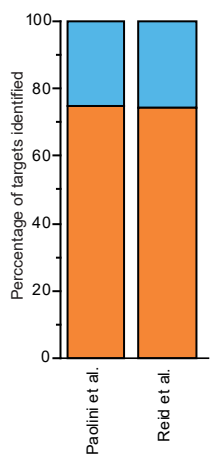
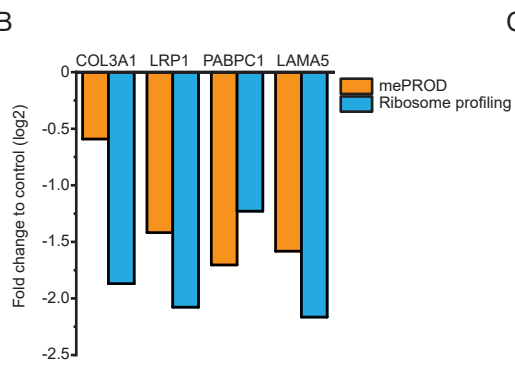


Figure S3

A



B



C

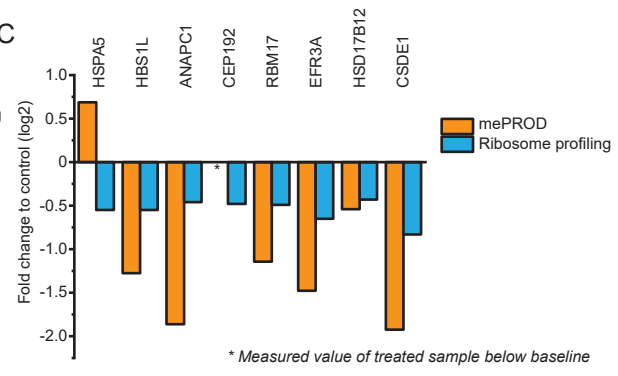


Figure S4

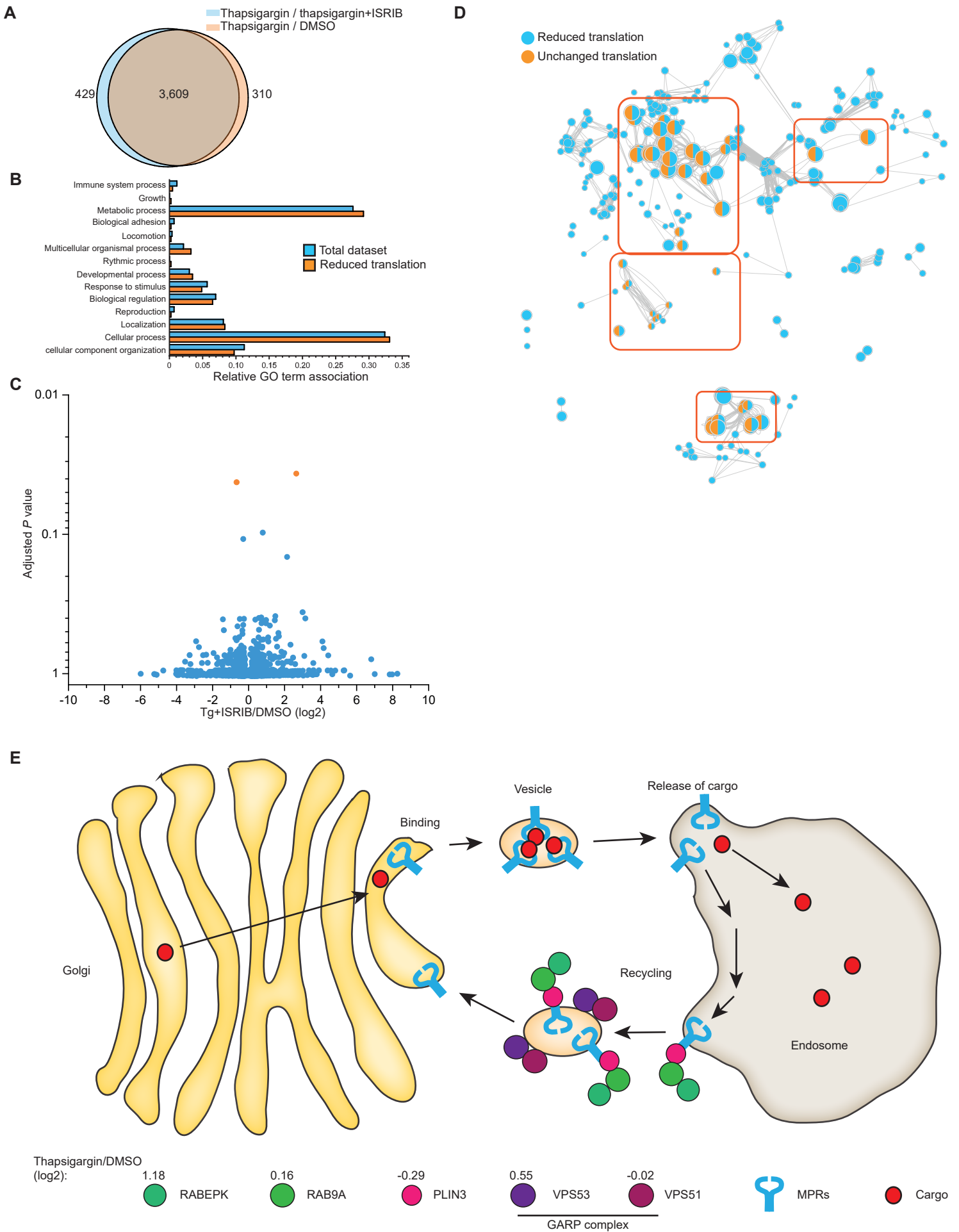


Figure S5

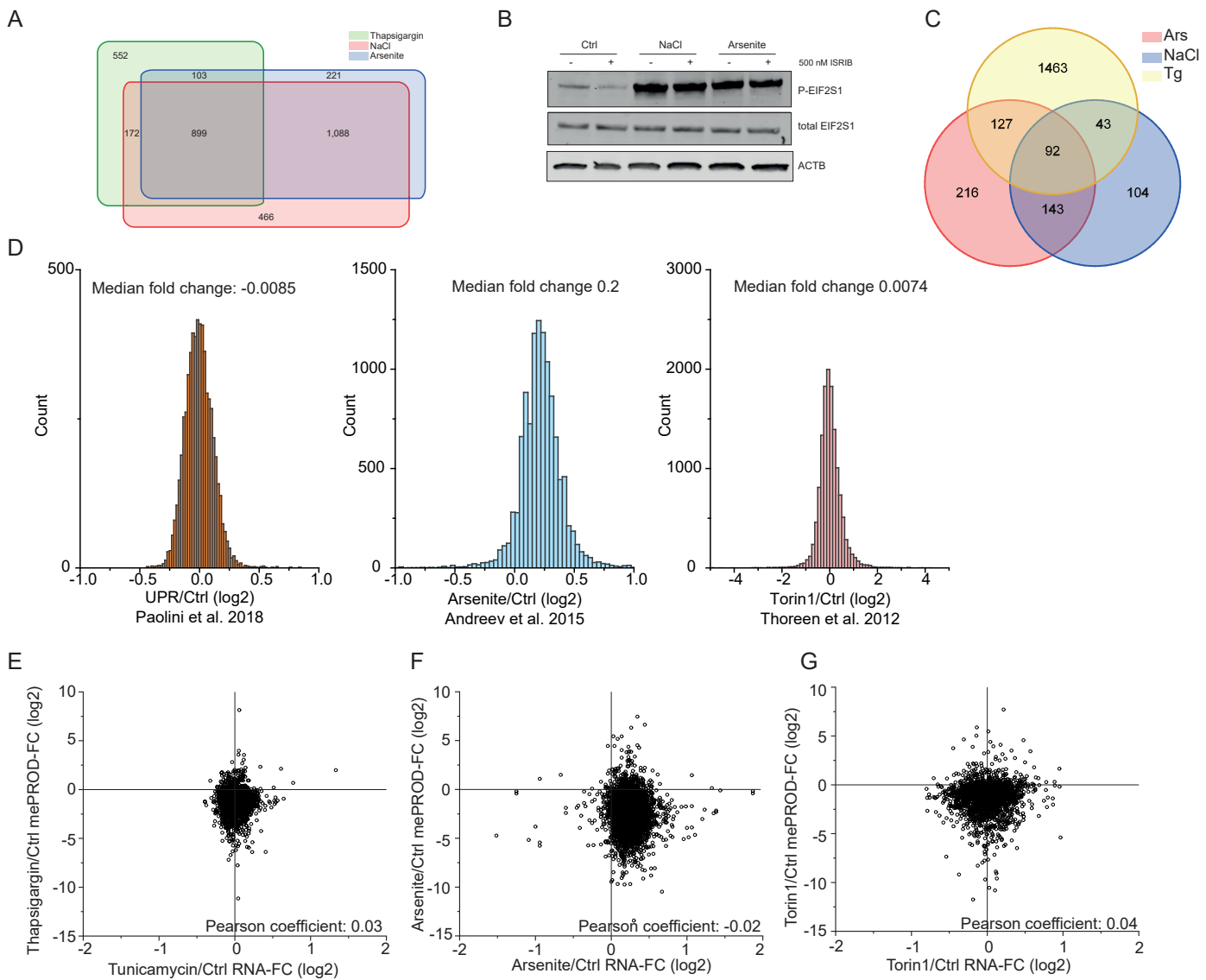




Figure S6

